ARTIFACT SHEET

Enter artifact number below. Artifact number is application number + artifact type code (see list below) + sequential letter (A, B, C ...). The first artifact folder for an artifact type receives the letter A, the second B, etc.. Examples: 59123456PA, 59123456PB, 59123456ZA, 59123456ZB

10/631999 CA

Indicate quantity of a single type of artifact received but not scanned. Create individual artifact folder/box and artifact number for each Artifact Type.

☐ CD(s) containing computer program listing
Doc Code: Computer Artifact Type Code: P

☑ Stapled Set(s) of Extra Color Drawings/Photographs
Doc Code: Artifact Artifact Type Code: C

☐ CD(s) containing pages of specification ☐ and/or sequence listing ☐
Doc Code: Artifact Artifact Type Code: S

☐ CD(s) with content unspecified
Doc Code: Artifact Artifact Type Code: U

☐ Microfilm(s)
Doc Code: Artifact Artifact Type Code: F

☐ Video tape(s)
Doc Code: Artifact Artifact Type Code: V

☐ Model(s)
Doc Code: Artifact Artifact Type Code: M

☐ Bound Document(s)
Doc Code: Artifact Artifact Type Code: B

☐ Other, description: _____
Doc Code: Artifact Artifact Type Code: Z

19. C. T. Chen *et al.*, *Phys. Rev. B* **48**, 642 (1993).
20. D. Spanke *et al.*, *Phys. Rev. B* **58**, 5201 (1998).
21. S. S. P. Parkin *et al.*, *J. Appl. Phys.* **85**, 5828 (1999).
22. F. Nolting *et al.*, *Nature* **405**, 767 (2000).
23. A. Scholl *et al.*, *Science* **287**, 1014 (2000).
24. K. Koike, K. Hayakawa, *Jpn. J. Appl. Phys.* **23**, L187 (1984).
25. J. Unguris, G. Hembree, R. J. Celotta, D. T. Pierce, *J. Microsc.* **139**, RP1 (1985).
26. H. P. Oepen, J. Kirschner, *Scanning Microsc.* **5**, 1 (1991).
27. R. Allenspach, *J. Magn. Magn. Mat.* **129**, 160 (1994).
28. M. R. Scheinfein, J. Unguris, M. H. Kelley, D. T. Pierce, R. J. Celotta, *Rev. Sci. Instrum.* **61**, 2501 (1990).
29. J. Barnes, L. Mei, B. M. Lairson, F. B. Dunning, *Rev. Sci. Instrum.* **70**, 246 (1999).
30. D. L. Abraham, H. Hopster, Phys.Rev. Lett. **58**, 1352 (1987).
31. H. Pinkvos, H. Poppa, E. Bauer, J. Hurst, *Ultramicroscopy* **47**, 339 (1992).
32. T. Duden, E. Bauer, *Phys. Rev. B* **59**, 474 (1999).
33. R. Wiesendanger, H.-J. Güntherodt, G. Güntherodtt, R. J. Gambino, R. Ruf, *Phys. Rev. Lett.* **65**, 247 (1990).
34. M. Johnson, J. Clarke, *J. Appl. Phys.* **67**, 6141 (1990).
35. S. F. Alvarado, *J. Appl. Phys.* **73**, 5816 (1993).
36. W. H. Rippard, R. A. Buhrman, *Appl. Phys. Lett.* **75**, 1001 (1999).
37. W. J. Kaiser, L. D. Bell, *Phys. Rev. Lett.* **60**, 1406 (1988).
38. V. P. LaBella *et al.*, *Science* **292**, 1518 (2001).
39. J. Wittborn, K. V. Rao, J. Nogués, I. K. Schuller, *Appl. Phys. Lett.* **76**, 2931 (2000).
40. S. Heinze *et al.*, *Science* **288**, 1805 (2000).
41. M. Bode, M. Getzlaff, R. Wiesendanger, *Phys. Rev. Lett.* **81**, 4256 (1998).
42. S. Blügel, M. Weinert, P. H. Dederichs, *Phys. Rev. Lett.* **60**, 1077 (1988).
43. M. Bode, O. Pietzsch, A. Kubetzka, S. Heinze, R. Wiesendanger, *Phys. Rev. Lett.* **86**, 2142 (2001).
44. W. K. Hiebert, A. Stankiewicz, M. R. Freeman, *Phys. Rev. Lett.* **79**, 1134 (1997).
45. D. D. Awschalom, J.-M. Halbout, S. von Molnar, T. Siegrist, F. Holtzberg, *Phys. Rev. Lett.* **55**, 1128 (1985).
46. Y. Acremann *et al.*, *Science* **290**, 492 (2000).
47. B. C. Choi, M. Belov, W. K. Hiebert, G. E. Ballentine, M. R. Freeman, *Phys. Rev. Lett.* **86**, 728 (2001).
48. T. M. Crawford, T. J. Silva, C. W. Teplin, C. T. Rogers, *Appl. Phys. Lett.* **74**, 3386 (1999).
49. J. Reif, J. C. Zink, C. M. Schneider, J. Kirschner, *Phys. Rev. Lett.* **67**, 2878 (1991).
50. F. Sirotti *et al.*, *J. Appl. Phys.* **83**, 1563 (1998).
51. M. Bonfim *et al.*, *Phys. Rev. Lett.* **86**, 3646 (2001).
52. J. M. Kikkawa, D. D. Awschalom, *Nature* **397**, 139 (1999).
53. W. Weber, S. Riesen, H. C. Seigmann, *Science* **291**, 1015 (2001).
54. E. O. Wilson, *Consilience: the unity of knowledge* (Knopf, New York, 1998).
55. K. Nakamura *et al.*, *Phys. Rev. B* **56**, 3218 (1997).
56. D. Rugar, C. S. Yannoni, J. A. Sidles, *Science* **264**, 1560 (1994).
57. We thank many colleagues for discussions and we thank G. Nunes and J. Beamish for comments on the manuscript. Supported by Natural Sciences and Engineering Research Council, Canadian Institute for Advanced Research, Informatics Circle of Research Excellence, and the Canada Research Chairs.

REVIEW

Spintronics: A Spin-Based Electronics Vision for the Future

S. A. Wolf,[1,2]* D. D. Awschalom,[3] R. A. Buhrman,[4] J. M. Daughton,[5] S. von Molnár,[6] M. L. Roukes,[7] A. Y. Chtchelkanova,[8] D. M. Treger[8]

This review describes a new paradigm of electronics based on the spin degree of freedom of the electron. Either adding the spin degree of freedom to conventional charge-based electronic devices or using the spin alone has the potential advantages of nonvolatility, increased data processing speed, decreased electric power consumption, and increased integration densities compared with conventional semiconductor devices. To successfully incorporate spins into existing semiconductor technology, one has to resolve technical issues such as efficient injection, transport, control and manipulation, and detection of spin polarization as well as spin-polarized currents. Recent advances in new materials engineering hold the promise of realizing spintronic devices in the near future. We review the current state of the spin-based devices, efforts in new materials fabrication, issues in spin transport, and optical spin manipulation.

Until recently, the spin of the electron was ignored in mainstream charge-based electronics. A technology has emerged called spintronics (spin transport electronics or spin-based electronics), where it is not the electron charge but the electron spin that carries information, and this offers opportunities for a new generation of devices combining standard microelectronics with spin-dependent effects that arise from the interaction between spin of the carrier and the magnetic properties of the material.

Traditional approaches to using spin are based on the alignment of a spin (either "up" or "down") relative to a reference (an applied magnetic field or magnetization orientation of the ferromagnetic film). Device operations then proceed with some quantity (electrical current) that depends in a predictable way on the degree of alignment. Adding the spin degree of freedom compared with conventional semiconductor devices.

Major challenges in this field of spintronics that are addressed by experiment and theory include the optimization of electron spin lifetimes, the detection of spin coherence in nanoscale structures, transport of spin-polarized carriers across relevant length scales and heterointerfaces, and the manipulation of both electron and nuclear spins on sufficiently fast time scales. In response, recent experiments suggest that the storage time of quantum information encoded in electron spins may be extended through their strong interplay with nuclear spins in the solid state. Moreover, optical methods for spin injection, detection, and manipulation have been developed that exploit the ability to precisely engineer the coupling between electron spin and optical photons. It is envisioned that the merging of electronics, photonics, and magnetics will ultimately lead to new spin-based multifunctional devices such as spin-FET (field effect transistor), spin-LED (light-emitting diode), spin RTD (resonant tunneling device), optical switches operating at terahertz frequency, modulators, encoders, de-

[1]Defense Advanced Research Projects Agency (DARPA), 3701 North Fairfax Drive, Arlington, VA 22203, USA. [2]Naval Research Laboratory, Washington, DC 20375, USA. [3]University of California, Department of Physics, Santa Barbara, CA 93106, USA. [4]Cor-

degree of freedom in semiconductors, semiconductor heterostructures, and ferromagnets, the potential for high-performance spin-based electronics will be excellent. The most interesting devices will probably be those that we have not even contemplated here!

Current Status of Spin-Based Electronic Devices

The discovery in 1988 of the giant magnetoresistive effect (GMR) is considered the beginning of the new, spin-based electronics (*1*, *2*). GMR is observed in artificial thin-film materials composed of alternate ferromagnetic and nonmagnetic layers. The resistance of the material is lowest when the magnetic moments in ferromagnetic layers are aligned and highest when they are antialigned. The current can either be perpendicular to the interfaces (CPP) or can be parallel to the interfaces (CIP). New materials operate at room temperatures and exhibit substantial changes in resistivity when subjected to relatively small magnetic fields (100 to 1000 Oe). For a detailed review of GMR, see (*3*).

A spin valve (Fig. 1A), a GMR-based device, has two ferromagnetic layers (alloys of nickel, iron, and cobalt) sandwiching a thin nonmagnetic metal (usually copper), with one of the two magnetic layers being "pinned"; i.e., the magnetization in that layer is relatively insensitive to moderate magnetic fields (*4*). The other magnetic layer is called the "free" layer, and its magnetization can be changed by application of a relatively small magnetic field. As the magnetizations in the two layers change from parallel to antiparallel alignment, the resistance of the spin valve rises typically from 5 to 10%. Pinning is usually accomplished by using an antiferromagnetic layer that is in intimate contact with the pinned magnetic layer. The two films form an interface that acts to resist changes to the pinned magnetic layer's magnetization. Recently, the simple pinned layer was replaced with a synthetic antiferromagnet: two magnetic layers separated by a very thin (~10 Å) nonmagnetic conductor, usually ruthenium (*5*). The magnetizations in the two magnetic layers are strongly antiparallel coupled and are thus effectively immune to outside magnetic fields. This structure improves both stand-off magnetic fields and the temperature of operation of the spin valve. The second innovation is the nano-oxide layer (NOL) formed at the outside surface of the soft magnetic film. This layer reduces resistance due to surface scattering (*6*), thus reducing background resistance and thereby increasing the percentage change in magnetoresistance of the structure.

A magnetic tunnel junction (MTJ) (Fig. 1B) (*7*, *8*) is a device in which a pinned layer and a free layer are separated by a very thin insulating layer, commonly aluminum oxide. The tunneling resistance is modulated by magnetic field in the same way as the resistance of a spin valve is, exhibits 20 to 40% change in the magnetoresistance, and requires a saturating magnetic field equal to or somewhat less than that required for spin valves. Because the tunneling current density is usually small, MTJ devices tend to have high resistances.

Applications for GMR and MTJ structures are expanding. Important applications include magnetic field sensors, read heads for hard drives, galvanic isolators, and magnetoresistive random access memory (MRAM). General purpose GMR sensors have been introduced in the past 5 years (*9*), and several companies are producing GMR sensors for internal consumption. No commercial sensor using MTJ structures are available, but one is under development (*10*).

GMR spin valve read heads are dominating applications in hard drives. Although some alternative configurations have been proposed, nearly all commercial GMR heads use the spin valve format as originally proposed by IBM (*11*). There has been development interest in MTJ and GMR multilayers for read head applications, but no important products have emerged yet. The magnetoresistance of spin valves has increased markedly from about 5% in early heads to about 15 to 20% today, using synthetic antiferromagnets and NOLs. As hard drive storage densities approach 100 Gbits per square inch, sensor stripe widths are approaching 0.1 μm and current densities are becoming very high. It is unclear if the conventional spin valve read head sensitivity can be extended to those levels or if a new form of read head will have to be introduced.

The GMR-based galvanic isolator (Fig. 2A) is a combination of an integrated coil and a GMR sensor on an integrated circuit chip. GMR isolators introduced in 2000 eliminate ground noise in communications between electronics blocks, thus performing a function similar to that of opto-isolators—providing electrical isolation of grounds between electronic circuits. The GMR isolator is ideally suited for integration with other communications circuits and the packaging of a large number of isolation channels on a single chip. Figure 2B shows a simple single-channel GMR isolator composed of a driver chip and a receiver chip in an 8 pin. More complex multichannel, bidirectional isolators are currently in production. The speed of the GMR isolator is currently 10 times faster than today's opto-isolators and can eventually be 100 times faster, with the principal speed limitations being the switching speed of the magnetic materials and the speed of the associated electronics.

MRAM uses magnetic hysteresis to store data and magnetoresistance to read data. GMR-based MTJ (*12*, *13*) or pseudospin valve (*14*) memory cells are integrated on an integrated circuit chip and function like a static semiconductor RAM chip with the added feature that the data are retained with power off. Potential advantages of the MRAM compared with silicon electrically erasable programmable read-only memory (EEPROM) and flash memory are 1000 times faster write times, no wearout with write cycling (EEPROM and flash wear out with about 1 million write cycles), and lower energy for writing. MRAM data access times are about 1/10,000 that of hard disk drives. MRAM is not yet available commercially, but production of at least 4-MB MRAM is anticipated in 2 to 3 years.

In just a few years, we have seen devices develop very rapidly. Several possible structures have suggested further improvements in magnetoresistance effect (*15*–*17*), from the 15 to 40% available today in GMR and MTJ structures, to hundreds of percent changes (at room temperature) with the new materials or structures, with the ultimate promise of "on-off" devices controlled by magnetism.

New Materials for Spintronics Applications

The search for material combining properties of the ferromagnet and the semiconductor has been a long-standing goal but an elusive one because of differences in crystal structure and chemical bonding (*18*, *19*). The advantages of

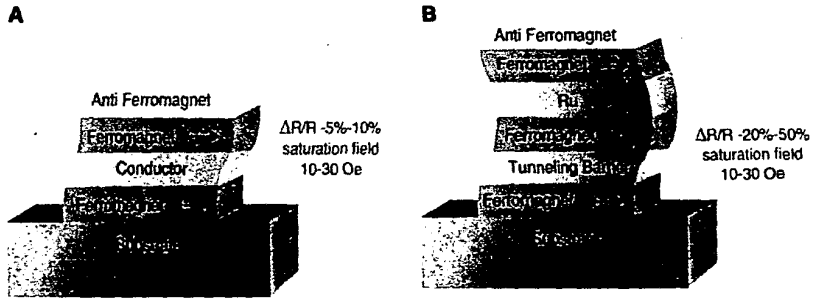

Fig. 1. Spin-dependent transport structures. (**A**) Spin valve. (**B**) Magnetic tunnel junction.

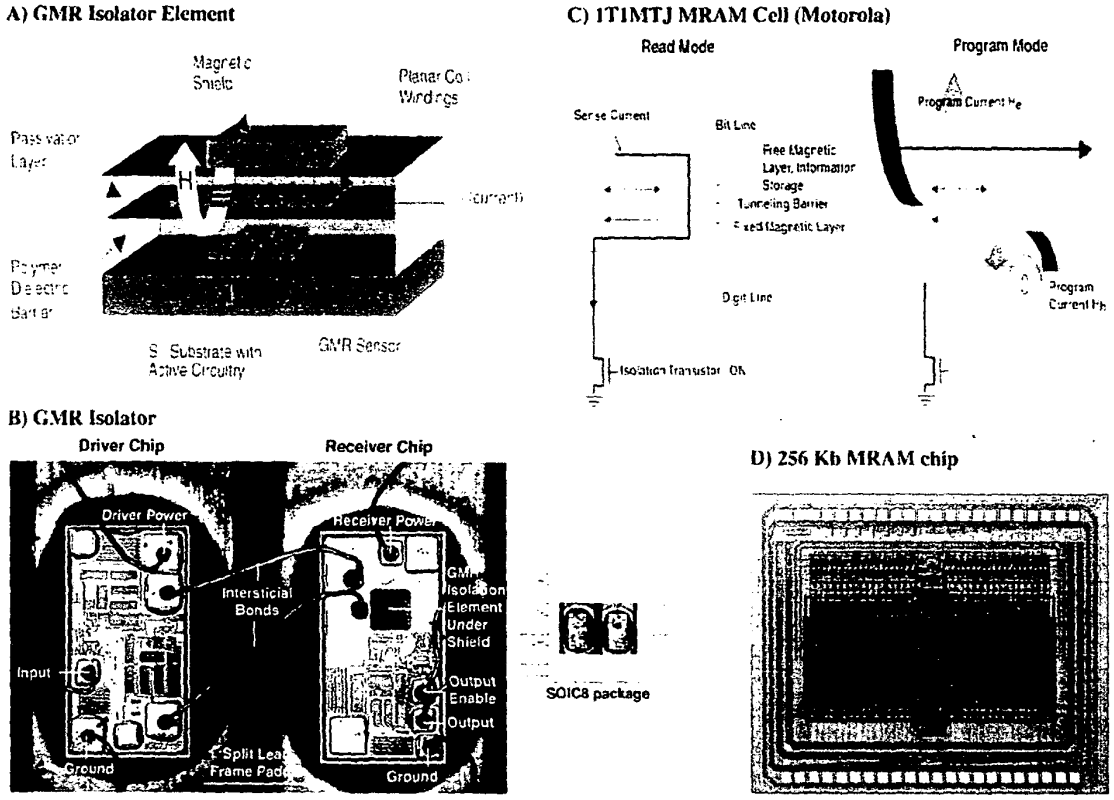

Fig. 2. (A to D) Device applications. A description of (C) is given in (*13*). [(B) courtesy of NVE; (D) courtesy of Motorola]

ferromagnetic semiconductors (FS) is their potential as spin-polarized carrier sources and easy integration into semiconductor devices. The ideal FS would have Curie temperatures above room temperature and would be able to incorporate not only p-type, but also n-type dopants. The Eu chalcogenides, the most thoroughly studied early magnetic semiconductors, in which the magnetic species (Eu^{2+}) resides on every lattice site, failed in the practical sense, because their ferromagnetic transition temperatures, T_C, were much lower than room temperature (*20*) with little hope of great improvement. The discovery of ferromagnetic order temperatures as high as 110 K in III-V–based diluted magnetic semiconductors (DMS) (*21*) (alloys in which some atoms are randomly replaced by magnetic atoms, such as Mn^{2+}) has generated much attention. There are theoretical predictions for T_C's above room temperature in several classes of these materials (*22*). And the discovery of electronically controlled magnetism (*23*) was recently reported. To achieve large spin polarization in semiconductors, the Zeeman splitting of the conduction (valence) band must be greater than the Fermi energy, E_F, of the electrons (holes). In concentrated materials, this occurs easily because the net magnetization upon ordering is proportional to the concentration of magnetic species. Figure 3A depicts this situation for doped EuS, where the change (Zeeman) splitting is ~0.3 eV (*24*) and an estimate of E_F based on 10^{20} cm^{-3} free carriers is ~0.15 eV. Externally applied magnetic fields may be necessary to produce large polarization in DMS where the Mn content is generally low (~5%) and may be limited by phase separation while the carrier concentrations are high (~10^{20} cm^{-3}).

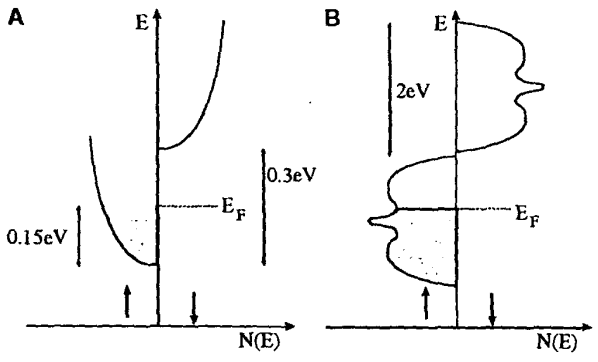

Fig. 3. (A) Schematic densities of states $N(E)$ for a concentrated magnetic semiconductor below T_C (*24*). (B) Schematic densities of states $N(E)$ for the half-metallic ferromagnet CrO_2 (*118*, *119*). Note that the energy scale is almost 10 times larger in (B).

Another approach is to search for new materials that exhibit large carrier spin polarization. Candidates include ferromagnetic oxides and related compounds, many of which are predicted to be "half-metallic" (*25*). The Fermi level intersects only one of the two spin bands, whereas for the other the Fermi level resides in a band gap (see Fig. 3B). Thus, there are efforts to produce magnetic Heussler alloys (*26*) such as NiMnSb (T_C = 728 K), which has been used as an electrode in tunneling junctions (*27*). Other possibilities are CrO_2 (*28*), the only ferromagnetic metallic binary oxide, and various members of the mixed valence perovskites (*29*), e.g., $La_{.70}Sr_{.30}MnO_3$, and Fe_3O_4, which, according to photoemission data (*30*), have com-

pletely spin-polarized electrons at the Fermi energy at room temperature. Worledge and Geballe have demonstrated, by spin-polarized tunneling, that the spin polarization is $P = +72\%$ for a variety of deposition conditions measured at 0.3 K (*31*). This is relatively consistent with earlier temperature-dependent spin-resolved photoemission at low temperatures (*32*); however, the data also show that this polarization decreases almost to zero near and above room temperature, indicating that the manganites will not provide spin-polarized sources for room temperature applications. A recent study of nanocontact magnetoresistance of half-metallic oxide, Fe_3O_4, however, has also been interpreted in terms of very high spin polarization of the transport carriers (*33*). Many of these oxides have been investigated (*34*) through Andreev reflection spectroscopy and yield high (above 70%) carrier spin polarization values at low temperature. The record is claimed for CrO_2 (*35*) with >96% polarization, albeit at liquid He temperatures. Finally, MnAs, with T_C near room temperature (*36*), and MnSb, which, in granular form on GaAs substrates, have a world record magnetoresistance at room temperature (*37*), are being investigated actively both in the United States and Japan to determine their spin polarization.

The development of new materials for spintronics applications continues to grow at a rapid pace. Using combinatorial synthesis methods, Japanese researchers have discovered room temperature ferromagnetism in laser-ablated 6 to 8% Co-doped TiO_2 having the anatase structure (*38*). This material is transparent to visible light and, consequently, may be of particular importance in optoelectronic applications. Zincblende CrSb/GaAs/CrSb epilayers have been confirmed to be room temperature ferromagnets (*39*). $Mn_{11}Ge_8$ crystals, which are known to have T_C's near room temperature (*40*), are currently being prepared nonstoichiometrically in thin-film form (*41*). Finally, we note the surprisingly high T_C of La-doped CaB_6 (*42*) (which contains no magnetic species). As Tromp *et al.* pointed out recently (*43*), this is a new semiconducting material for spin electronics. It is apparent that the development of new materials will continue to be a major part of any program on spintronics.

To systematically develop and characterize magnetoelectronic materials and devices, one needs imaging and measuring techniques allowing spatial resolution of structural dimensions of the samples and having sensitivity to detect very small total magnetic moments. Most of the techniques have, to date, provided information only about the time-averaged magnetic properties or dynamics for processes slower than roughly the microsecond scale. For the iterative refinement of advanced magnetic materials and devices, one has to be able to measure spin relaxation in magnetic nanostructures and the precise details of magnetization reversal. For more details about magnetic imaging techniques, see Freeman and Choi's review in this issue (*44*).

Electrical Spin Injection and Spin Transport

Successful application of the wide range of possible spin-dependent phenomena in semiconductor systems requires effective and efficient techniques for the electrical injection of strongly spin-polarized currents (spin currents), as well as electrical detection of such spin currents. For the semiconductor case, this detection could possibly occur either within the semiconductor or upon the current exiting the semiconductor system, depending on the device design. For practical applications, it is of course highly desirable that the generation, injection, and detection of such spin currents be accomplished without requiring the use of extremely strong magnetic fields and that these processes be effective at or above room temperature. The use of ferromagnetic metallic electrodes appears to be essential for most practical all-electrical spin-based devices until and unless useful FS are developed.

Ohmic injection. In a ferromagnetic metal (FM), the electrical conductivity of the majority spin (spin-up) electrons differs substantially from minority spin (spin-down), resulting in a spin-polarized electric current. The most straightforward approach to spin injection is the formation of an ohmic contact between an FM and a semiconductor, anticipating a spin-polarized current in the semiconductor. However, typical metal-semiconductor ohmic contacts result from heavily doping the semiconductor surface, leading to spin-flip scattering and loss of the spin polarization. The research was initially focused on FM contacts to InAs, one of the few semiconductors with an ideal, abrupt interface to a transitional metal, and the result was expected to be an ohmic, Schottky-barrier–free contact. In spite of much effort (*45*, *46*), spin injection from FM-InAs ohmic contacts has resulted in small effects or was obtained by indirect methods or both. To date, 4.5% spin-polarized ohmic injection from FM into semiconductor at $T < 10$ K (*47*) has been reported.

Following up on earlier studies (*48*–*51*) of diffusive spin transport, recent work by Schmidt *et al.* (*52*) has pointed out a fundamental problem regarding ohmic spin injection across ideal FM-nonferromagnet (NFM) interfaces. The effectiveness of the spin injection depends on the ratio of the (spin-dependent) conductivities of the FM and NFM electrodes, σ_F and σ_N, respectively. When $\sigma_F \leq \sigma_N$, as in the case of a typical metal, then efficient and substantial spin injection can occur, but when the NFM electrode is a semiconductor, $\sigma_F \gg \sigma_N$ and the spin-injection efficiency will be very low. Only for a ferromagnet where the conduction electrons are nearly 100% spin polarized can efficient spin injection be expected in diffusive transport. There are a number of materials that apparently have such half-metal ferromagnet properties (*25*, *53*), although these are challenging materials with which to work.

Johnson and co-workers have proposed and pursued (*54*–*57*) an approach that may overcome this obstacle to spin injection by taking advantage of the splitting of the spin degeneracy of electrons confined in a semiconductor two-dimensional (2D) quantum well structure. The splitting is due to the spin-orbit effect that can arise from an asymmetry in the confining potential (*58*). The result can be an inducement of a nonequilibrium spin polarization if the 2D electron gas is carrying a current (*59*). However, as in the ohmic contact experiments, the small percentage change in device resistance that is observed with changes in ferromagnet orientation has led to suggestions of an alternative, local-Hall-effect explanation for the data and to other questions regarding this approach (*60*–*62*). At present, the feasibility and effectiveness of this current-induced spin polarization for spin injection appear to be unsettled.

Tunnel injection. Alvarado and Renaud (*63*), using a scanning tunneling microscope (STM) with a ferromagnetic tip, showed that a vacuum tunneling process can effectively inject spins into a semiconductor. A recent extension of this has examined the effect of surface structure on spin-dependent STM tunneling (*64*). The development of FM-insulator-FM tunnel junctions with high magnetoresistance has also demonstrated that tunnel barriers can result in the conservation of the spin polarization during tunneling, suggesting that tunneling may be a much more effective means for achieving spin injection than diffusive transport.

Recent theoretical work by Rashba (*65*) and Flatte and co-workers (*66*) has quantitatively developed the understanding of the potential effectiveness of tunnel injection. If the impedance of a barrier at an interface is sufficiently high, then the transport across that interface will be determined by the (spin-dependent) density of the electronic states of the two electrodes that are involved in the tunneling process. The current through the barrier is then sufficiently small that the electrodes remain in equilibrium and the relative (spin-dependent) conductivities of the electrodes play no substantial role in defining or limiting the spin-dependent transport across the interface. Thus, either a metal-insulator-semiconductor tunnel diode or a metal-semi-

conductor Schottky barrier diode that uses an FM electrode can be expected to be an effective means for injecting spins into a semiconductor system.

A number of groups have begun efforts on the epitaxial growth of ferromagnetic thin films on semiconductors with emphasis on forming abrupt, high-quality Schottky barriers. Much of this effort has concentrated on the growth of Fe and Fe-Co on GaAs (*67*, *68*). Zhu *et al.* (*68*) have recently reported a room temperature spin-injection efficiency of 2% with such an Fe-GaAs Schottky diode, with the injected spin polarization being detected by the degree of circular polarization of the electroluminescence (EL). Important aspects of EL detection of spin injection are both the size of the circularly polarized EL signal that depends on the magnetic orientation of the ferromagnetic electrode and the absence of any such dependence in photoluminescence measurements, which can rule out several possible measurement artifacts.

Ballistic electron injection. An alternative to tunnel injection is spin injection across ferromagnet-semiconductor interfaces in the ballistic regime, with the difference between the two spin conduction subbands of the ferromagnetic metal and the conduction band of the semiconductor determining the spin-dependent interfacial ballistic electron transmission probability. It is generally assumed that the transverse momentum of an incident electron is conserved, and this determines the ballistic transmission and reflection probabilities of the interface (*69*, *70*). Also, once a spin-polarized electron enters the semiconductor electrode, the probability that it will be elastically scattered back into the ferromagnetic injector must be very small. If the device design also involves, for example, the spin-dependent capture of an injected carrier by another ferromagnetic electrode, then transport through the semiconductor region must be fully ballistic. However, if the objective is simply efficient spin injection, a three-dimensional ballistic point contact between a ferromagnet and a semiconductor should be effective. Recent experiments with point contacts formed between ferromagnetic and nonferromagnetic metals have demonstrated the ballistic point-contact injection of high (>40%) spin-polarized currents into the NFM (*71*, *72*).

Hot electron injection. Another spin injection technique involves the use of spin-polarized "hot" electrons having energies that are much greater than E_F by tunnel-injecting electrons into a ferromagnetic layer at energies $\gg E_F$ (*73*–*75*). As the majority-spin and minority-spin electrons have much different inelastic mean free paths, hot electron passage through, for example, a 3-nm Co layer, is sufficient to result in a ballistic electron current that is more than 90% polarized (*75*). This highly polarized hot-electron current can then continue on to an underlying metal-semiconductor interface where a portion of the beam will enter the semiconductor, with the transmission probability being determined by energy and momentum constraints imposed by the band structure difference between the semiconductor and metal at the interface. If there is no substantial spin-flip scattering at the interface, then the ballistic electron current entering the semiconductor will be also very highly polarized (>90%) and the injection energy, relative to the bottom of the semiconductor conduction band, tunable through the tunnel injection bias. The disadvantage of hot electron injection is that the overall efficiency is low.

Spin detection. The most obvious approach to the electrical detection of spin populations in semiconductors is to use the spin-dependent transport properties of semiconductor-ferromagnet interfaces. Experimental efforts with this spin-valve detection scheme have used ohmic contacts for the spin collection electrode. But the same difficulties discussed above apply to spin collection, and it appears that for effective spin collection/detection, either a ballistic contact or a tunneling contact from the semiconductor to a ferromagnet will be required. If, however, for reasons of signal-to-noise, an efficient spin-dependent extraction of the injected spin-polarized current is required, then the tunnel barrier has to be sufficiently thin that (spin-dependent) tunneling transport into the ferromagnetic electrode is more probable than spin relaxation within the semiconductor (*65*). An alternative spin detection technique is a potentiometric measurement, with a ferromagnetic electrode, of the chemical potential of the nonequilibrium spin populations (*56*, *57*). With respect to the complete spin-transistor device, an extensive analysis by Tang *et al.* (*76*) has concluded that only for the case of ballistic transport throughout the device structure will the desired, electrical-field–tunable spin precession be detectable as polarized electrons transit through the semiconductor region. Moreover, they conclude, in accord with the initial suggestion of Datta and Das (*77*), that a very narrow, single- or few-electron channel device structure will be required.

Spin transport. Of particular interest to the spin transport theory in semiconductor systems has been the question as to whether the quasi-independent electron model can adequately account for the experimental results, or whether many-body, or correlated-electron processes are important. Flatte *et al.* (*66*) have extensively examined this issue in the diffusive transport regime and have concluded that an independent electron approach is quite capable of explaining measurements of spin lifetimes, particularly the room temperature measurements. Sham and colleagues (*78*, *79*) have been focusing on the very low temperature regime where collective electron processes may well be important in determining the spin relaxation rates and spin lifetimes, although experimental results in this regime are quite limited. On the device front, Flatte and Vignale (*80*) have considered the possibility of constructing unipolar electronic devices by using ferromagnetic semiconductor materials with variable magnetization directions. They have shown that such devices should behave very similarly to p-n diodes and bipolar transistors and suggest that they could be applicable for magnetic sensing, memory, and logic.

Spin transfer. Recently, experiments have demonstrated that the spin-polarized current that flows from one relatively thick, and hence fixed, ferromagnetic layer, through a nonmagnetic layer, to another thin-film "free" nanomagnet can by spin-dependent scattering of the polarized current (*81*–*83*) excite strong, uniform spin-wave precessional modes in the nanomagnet (*84*–*86*). In the absence of a strong external magnetic field, this spin-dependent scattering can also result in the reversal of the orientation of the magnetic moment of the free nanomagnet with the final orientation relative to the fixed layer being dependent on the direction of the current flow (*87*). This "spin-transfer" process opens up the possibility of new nanoscale devices for memory and other spin electronics applications (*88*). One application, in addition to direct current addressable magnetic memory, might be the use of spin transfer to excite a uniform spin wave in a nanomagnet and then to use this nanomagnet as a precessing spin filter to inject a coherent spin pulse into a semiconductor structure.

Optical Manipulation of Spin Coherence in Semiconductors and Nanostructures

Time-resolved optical experiments have revealed a remarkable resistance of electron spin states to environmental sources of decoherence in a wide variety of direct band-gap semiconductors (*93*). Optical pulses are used to create a superposition of the basis spin states defined by an applied magnetic field and follow the phase, amplitude, and location of the resulting electronic spin precession (coherence) in bulk semiconductors, heterostructures, and quantum dots. The data identify narrow ranges of doping concentrations where spin lifetimes in semiconductors are enhanced by orders of magnitude, culminating in the observation of spin lifetimes in bulk semiconductors that exceed 100 ns. In heterostructures and quantum dots, nanosecond dynamics persist to room temperature, providing pathways toward practical coherent quantum magnetoelectronics.

Coherent spin transport through semiconductors and interfaces. Understanding the fundamental properties of spin transport in the solid state is essential for the development of semiconductor-based spintronics. In analogy to conventional devices whose performance is characterized by carrier mobilities and lifetimes, spin mobilites and coherence times are figures of merit for spintronic devices. Recent theoretical work has shown that it is essential to consider the influence of electric fields induced by carrier motion to understand the motion of spin and that the room temperature spin coherence times in bulk and quantum well structures appear to be dominated by precessional decoherence due to spin-orbit coupling (*94*). These models describe how the low-field mobility and diffusion of spin packets depend sensitively on the doping and reveal new opportunities to control spin interactions by engineering strain and crystal orientation (*95*).

The spatial selectivity and temporal resolution of optical techniques have been used to monitor the decoherence and dephasing of electron spin polarization during transport not only through bulk semiconductors but also across heterojunctions in engineered structures. Data show that spin coherence is largely preserved as electron spins cross interfaces over a broad range of temperatures (Fig. 4) (*96*). A phase shift is imposed on the electron spins during the crossing that is set by the difference in electron g factors between the two materials and can be controlled with epitaxial growth techniques. Further measurements have established an increase in spin injection efficiency with bias-driven transport: Relative increases of up to 500% in electrically biased structures and 4000% in p-n junctions have been observed (*97*). On the basis of the extended spin lifetimes discovered previously, a new "persistent" spin conduction mode appears upon bias, sourcing coherent spin transfer for at least one to two orders of magnitude longer than in unbiased structures.

A deeper understanding of the effect of defects on spin coherence is clearly important for the development of spin-based electronics. In this context, the III-V semiconductor GaN is intriguing in that it combines a high density of charged threading dislocations with high optical quality, allowing optical investigation of the effects of momentum scattering on coherent electronic spin states. Despite an increase of eight orders of magnitude in the density of charged threading dislocations, studies reveal electron spin coherence times in GaN epilayers that reach ~20 ns at $T = 5$ K, with observable coherent precession at room temperature (*98*). Detailed investigations reveal a dependence on both magnetic field and temperature qualitatively similar to previous studies in GaAs, suggesting a common origin for spin relaxation in these systems. These experiments present promising opportunities for multifunctional devices such as spin transistors that combine memory and logic functions where the amplitude and phase of the net spin current can be controlled by either electric or magnetic fields in a wide variety of materials.

Magnetic doping in semiconductor heterostructures: integration of magnetics and electronics. As discussed in the section "New Materials for Spintronics Applications," magnetic doping with elements such as paramagnetic Mn^{2+} ions resulted in a wide variety of new physical phenomena in II-VI and III-V semiconductors. In II-VI systems, the Mn^{2+} ions act to boost the electron spin precession up to terahertz frequencies and exhibit optically induced coherent precession of the magnetic moments as well (*99*). The large electronic Zeeman splittings in magnetic II-VI semiconductors at low temperatures have enabled the design and operation of a prototype spintronic device: a spin-LED that shows a high spin polarization in applied magnetic fields of a few tesla (*100*, *101*). The concurrent development of spin-LEDs with recently discovered ferromagnetic III-V semiconductors [e.g., (Ga,Mn)As and (In,Mn)As] has led to remanent spin injection at zero applied field and operation at higher temperatures (albeit with a lower polarization efficiency) (*102*). For future devices, theoretical proposals suggest that the domains in a unipolar magnetic semiconducting film could be configured to produce transistor-like behavior, with potential applications in nonvolatile memory and reprogrammable logic. In some Mn-doped III-V materials, the presence of light drives the paramagnetic ions into ferromagnetic order, resulting in optically controlled ferromagnetism in semiconductors (Fig. 5) (*103*). Although this is currently a low-temperature effect, extension to higher temperature may have important applications in areas ranging from optical storage to photonically driven micromechanical elements. More recently, these materials have been used to show electric-field control of the ferromagnetism with a field-effect transistor structure (*23*). In complement to these classical approaches to spin-based devices, the introduction of coherent spins into ferromagnetic structures could lead to a new class of quantum

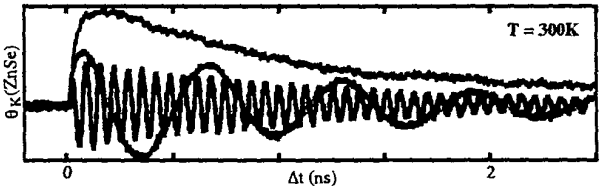

Fig. 4. Room temperature spin transport across a GaAs/ZnSe heterojunction. Kerr rotation with a probe energy of 2.8 eV detects coherent spins created in GaAs that cross the interface into ZnSe. Results are shown for electron spins precessing in magnetic field B = 0 T (purple curve), 0.025 T (pink curve), and 0.250 T (black curve). [Adapted from (*120*)]

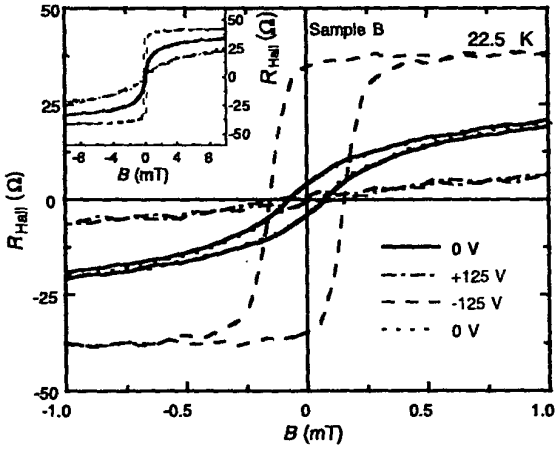

Fig. 5. Field effect control of hole-induced ferromagnetism in magnetic semiconductor (In,Mn)As field-effect transistors. Shown is magnetic field dependence of the sheet Hall resistance R_{Hall}, which is proportional to the magnetization of the magnetic semiconductor layer, as a function of the applied gate voltage V_G. R_{Hall} is used to measure the small magnetization of the channel. V_G controls the hole concentration in the magnetic semiconductor channel. Application of $V_G = 0$, +125, and −125 V results in qualitatively different field dependence of R_{Hall} measured at 22.5 K. When holes are partially depleted from the channel ($V_G = +125$ V), a paramagnetic response is observed (blue dash-dotted line), whereas a clear hysteresis at low fields (< 0.7 mT) appears as holes are accumulated in the channel ($V_G = -125$ V, red dashed line). Two R_{Hall} curves measured at $V_G = 0$ V before and after application of ±125 V (black solid line and green dotted line, respectively) are virtually identical, showing that the control of ferromagnetism can be done isothermally and reversibly. (Inset) The same curves shown at higher magnetic fields. [Adapted from (*23*)]

magnetoelectronics. As an example, some proposed quantum computation schemes rely on the controllable interaction of coherent spins with ferromagnetic materials to produce quantum logic operations (*104*).

Optical control of nuclear spins. Nuclear spins have been proposed as candidates for storing both classical and quantum information because of spin lifetimes that exceed those of electrons by at least several orders of magnitude and the degree of control provided by conventional nuclear magnetic resonance (NMR) techniques. For future applications that exploit delocalized electrons, the hyperfine interaction in III-V semiconductors has been directly probed through a resonant technique based on periodically excited electron spin polarization (*105*). Time-resolved measurements of electron spin precession have provided unambiguous signatures of all-optical NMR in modulation-doped GaAs quantum wells and represent the spatial focusing of NMR mechanisms to the nanometer length scale (*106*). More recently, there is experimental evidence that ferromagnetic materials can be used to imprint nuclear spins in semiconductors (*107*), thereby offering an additional pathway for manipulating and storing information at the atomic scale.

Artificial atoms in the solid state: quantum dots. It has been proposed that the spin of an electron confined to quantum dots is a promising candidate for quantum bits and that arrays of quantum dots can be used in principle to implement a large-scale quantum computer (*108*, *109*) Quantum operations in these proposals are provided by the coupling of electron spins in neighboring quantum dots by an exchange interaction between them. This interaction can be switched by applying controlled gate voltage pulses, thus allowing realization of fundamental quantum gates such as the exclusive OR. The read-out of such a spin qubit can be performed efficiently as a spin-polarized electric current passing through the dot (*110*) or optically through integration in solid state microcavities (*111*). Alternatively, qubit rotations can be implemented by local electrostatic shifting of the electron into a region with a different effective magnetic field, such as occurs at heterointerfaces and in magnetic semiconductor structures.

Direct optical manipulation of charge-based coherent wave packets has been achieved in individual quantum dots (*112*). Many proposals exist for a hybrid technique of spin-to-charge conversion that may be desirable for combining the longer spin coherent lifetimes with the sensitivity of charge detection. Recent experiments have revealed that the transverse and longitudinal relaxation times for electron spins in insulating quantum dots are in the nanosecond regime and offer promise for their utilization as computing elements in quantum electronics (*92*, *113*). The challenge of performing a suitably large number of qubit rotations within the spin coherence time has been addressed by a new technique developed in quantum wells that produces rotations of electron spins on 100-fs time scales (*114*). In these experiments, intense laser pulses energetically tuned below the semiconductor band gap generate a light-induced effective magnetic field through the optical Stark effect and successfully operate on quantum-confined electron spin states.

Another proposal (*115*) suggests that individual phosphorous nuclei embedded in silicon may be treated as quantum bits whose entanglement proceeds through the hyperfine interaction with localized electron spins and with a gate-controlled exchange interaction between neighboring spins (*108*). Along with a related scheme applied to Si-Ge compounds (*116*), the choice of group-IV semiconductors has the advantage of reduced spin-orbit coupling that could lead to even longer spin coherence times (*117*).

Outlook

To continue the rapid pace of discoveries, considerable advances in our basic understanding of spin interactions in the solid state along with developments in materials science, lithography, minaturization of optoelectronic elements, and device fabrication are necessary. The progress toward understanding and implementing the spin degree of freedom in metallic multilayers and, more recently, in semiconductors is gaining momentum as more researchers begin to address the relevant challenges from markedly different viewpoints. Spintronic read head sensors are already impacting a multibillion dollar industry and magnetic random access memory using metallic elements will soon impact another multibillion dollar industry. With contributions from a diversity of countries and fields including biology, chemistry, physics, electrical engineering, computer science, and mathematical information theory, the rapidly emerging field of spintronics promises to provide fundamentally new advances in both pure and applied science as well as have a substantial impact on future technology.

References and Notes

1. M. Baibich *et al.*, *Phys. Rev. Lett.* **61**, 2472 (1988).
2. J. Barnas, A. Fuss, R. Camley, P. Grunberg, W. Zinn, *Phys. Rev. B* **42**, 8110 (1990).
3. G. Prinz, *Science* **282**, 1660 (1998).
4. B. Dieny *et al.*, *J. Appl. Phys.* **69**, 4774 (1991).
5. S. Parkin, D. Mauri, *Phys. Rev. B* **44** 7131 (1991).
6. W. F. Egelhoff jr. *et al.*, *J. Vac. Sci. Technol. B* **17**, 1702 (1999).
7. J. S. Moodera, L. R. Kinder, T. M. Wong, R. Meservey, *Phys. Rev. Lett.* **74**, 3273 (1995).
8. T. Miyazaki *et al.*, *J. Magn. Magn. Mater.* **151**, 403 (1995).
9. J. Daughton, J. Brown, R. Beech, A. Pohm, W. Kude, *IEEE Trans. Magn.* **30**, 4608 (1994).
10. M. Tondra, J. Daughton, D. Wang, A. Fink, *J. Appl. Phys.* **83**, 6698 (1998).
11. C. Tsang *et al.*, *IEEE Trans. Magn.* **30**, 3801 (1994).
12. R. E. Scheuerlein *et al.*, 2000 IEEE ISSCC Digest of Technical Papers Cat. No.00CH37056, 128 (2000).
13. P. Naji, M. Durlam, S. Tehrani, J. Cader, M. DeHerrera, paper presented at the International Solid State Circuits Conference (2001).
14. R. Katti *et al.*, Paper FD-04 presented at the 8th Joint MMM-Intermag Conference, San Antonio, TX, 7 to 11 January 2001.
15. J. J. Versluijs, J. M. D. Coey, *J. Magn. Magn. Mater.* **226**, 688 (2001).
16. H. Akinaga, M. Mizuguchi, K. Ono, M. Oshima, *Appl. Phys. Lett.* **76**, 357 (2000).
17. M.-H. Jo, N. D. Mathur, N. K. Todd, M. G. Blamire, *Phys. Rev. B* **61**, R14905 (2000).
18. M. Tanaka, *J. Cryst. Growth* **201/202**, 660 (1999).
19. G. Prinz, K. Hathaway, *Phys. Today* **48**, 24 (1995).
20. S. Methfessel, D. C. Mattis, *Handb. Phys.* **18**, 389 (1968).
21. H. Ohno *et al.*, *Appl. Phys. Lett.* **69**, 363 (1996).
22. T. Dietl *et al.*, *Science* **287**, 1019 (2000).
23. H. Ohno *et al.*, *Nature* **408**, 944 (2000).
24. S. von Molnár, *IBM J. Res. Dev.* **14**, 269 (1970).
25. R. A. de Grot *et al.*, *Phys. Rev. Lett.* **50**, 2024 (1983).
26. J. W. Dong *et al.*, *Appl. Phys. Lett.* **75**, 1443 (1999).
27. C. T. Tanaka, J. Nowak, J. S. Moodera, *J. Appl. Phys.* **86**, 6239 (1999).
28. S. M. Watts *et al.*, *Phys. Rev B* **61**, 9621 (2000).
29. J. M. D. Coey, M. Viret, S. von Molnár, *Adv. Phys.* **48**, 169 (1999).
30. F. J. Jedema, A. T. Filip, B. J. van Wees, *Nature* **410**, 345 (2001).
31. D. C. Worledge, T. H. Geballe, *Appl. Phys. Lett.* **76**, 900 (2000).
32. J.-H. Park *et al.*, *Phys. Rev. Lett.* **81**, 1953 (1998).
33. J. J. Versluijs, M. A. Bari, J. M. D. Coey, *Phys. Rev. Lett.* **87**, 026601 (2001).
34. R. J. Soulen *et al.*, *Science* **282**, 85 (1998).
35. Y. Ji *et al.*, *Phys. Rev. Lett.* **86**, 5585 (2001).
36. C. P. Beam, D. S. Rodbell, *Phys. Rev.* **126**, 104 (1962).
37. H. Akinaga, M. Mizuguchi, K. Ono, M. Oshima, *J. Mag. Soc. Jpn.* **22**, 451 (2000).
38. Y. Matsumoto *et al.*, *Science* **291**, 854 (2001).
39. J. Zhao *et al.*, *Appl. Phys. Lett.* **79**, 2776 (2001).
40. N. Yamada *et al.*, *J. Phys. Soc. Jpn.* **55**, 3721 (1986).
41. Y. D. Park *et al.*, *Appl. Phys. Lett.* **78**, 2739 (2001).
42. D. P. Young *et al.*, *Nature* **397**, 412 (1999).
43. H. J. Tromp *et al.*, *Phys. Rev. Lett.* **87**, 016401 (2001).
44. M. Freeman, B.-C. Choi, *Science* **294**, 1484 (2001).
45. F. G. Monzon, M. Roukes, *J. Magn. Magn. Mater* **198-199**, 632 (1999).
46. S. Gardelis *et al.*, *Phys. Rev. B* **60**, 7764 (1999).
47. C.-M. Hu *et al.*, *Phys. Rev. B* **63**, 125333 (2001).
48. M. Johnson, R. H. Silsbee, *Phys. Rev. B* **35**, 4959 (1987).
49. P. C. van Son *et al.*, *Phys. Rev. Lett.* **58**, 2271 (1987)
50. T. Valet, A. Fert, *Phys. Rev. B* **48**, 7099 (1993).
51. S. Hershfield, H. L. Zhao, *Phys. Rev. B* **56**, 3296 (1997).
52. G. Schmidt *et al.*, *Phys. Rev. B* **62**, R4790 (2000).
53. K. P. Kamper *et al.*, *Phys. Rev. Lett.* **59**, 2788 (1988).
54. M. Johnson, *Phys. Rev B* **58**, 9635 (1998).
55. P. R. Hammar, B. R. Bennett, M. J. Yang, M. Johnson, *Phys. Rev. Lett.* **83**, 203 (1999).
56. P. R. Hammar, M. Johnson, *Phys. Rev. B* **61**, 7207 (2000).
57. M. Johnson, *Physica E* **10**, 472 (2001).
58. Y. A. Bychkov, E. I. Rashba, *Pis'ma Zh. Eksp. Teor. Fiz.* **39**, 66 (1984) [*JETP Lett.* **39**, 78 (1984)].
59. L. E. Vorob'ev *et al.*, *Pis'ma Zh. Eksp. Teor. Fiz* **29**, 485 (1979) [*JETP Lett.* **29**, 441 (1979)].
60. F. G. Monzon *et al.*, *Phys. Rev. Lett.* **84**, 5022 (2000).
61. B. J. Wees, *Phys. Rev. Lett.* **84**, 5023 (2000).
62. P. R. Hammar *et al.*, *Phys. Rev. Lett.* **84**, 5024 (2000).
63. S. F. Alvarado, Ph. Renaud, *Phys. Rev. Lett.* **68**, 1387 (1992).
64. V. LaBella *et al.*, *Science* **292**, 1518 (2001).

65. E. I. Rashba, *Phys. Rev. B* **62**, R16267 (2000).
66. M. E. Flatte, J. Byers, W. H. Hau, unpublished data.
67. L. C. Chen *et al.*, *J. Vac. Sci. Tech. B* **18**, 2057 (2000).
68. H. J. Zhu *et al.*, *Phys. Rev. Lett.* **87**, 016601 (2001).
69. G. Kirczenow, *Phys. Rev. B* **63**, 054422 (2001).
70. D. Grundler, *Phys. Rev. B* **63**, R161307 (2001).
71. S. K. Upadhyay *et al.*, *Phys. Rev. Lett.* **81**, 3247 (1998).
72. S. K. Upadhyay *et al.*, *Appl. Phys. Lett.* **74**, 3881 (1999).
73. D. Monsma *et al.*, *Phys. Rev. Lett.* **74**, 5260 (1995).
74. R. Jansen *et al.*, *J. Appl Phys.* **89**, 7431 (2001).
75. W. H. Rippard, R. A. Buhrman, *Phys. Rev. Lett.* **84**, 971 (2000).
76. H. X. Tang *et al.*, *Phys. Rev. B* **61**, 4437 (2000).
77. S. Datta, B. Das, *Appl. Phys. Lett.* **56**, 665 (1990).
78. L. J. Sham, T. Ostreich, *J. Lumin.* **87**, 179 (2000).
79. L. J. Sham, *J. Magn. Magn. Mat.* **200**, 219 (1999).
80. M. E. Flatte, G. Vignale, *Appl. Phys. Lett.* **78**, 1273 (2001).
81. L. Berger, *Phys. Rev. B* **54**, 9353 (1996).
82. J. C. Slonczewski, *J. Magn. Magn. Mater.* **159**, L1 (1996).
83. ———, *J. Magn. Magn. Mater.* **195**, L261 (1999).
84. M. Tsoi *et al.*, *Phys. Rev. Lett.* **80**, 4281 (1998) [erratum, *Phys. Rev. Lett.* **81**, 493 (1998)].
85. E. B. Myers, D. C. Ralph, J. A. Katine, R. N. Louie, R. A. Buhrman, *Science* **285**, 867 (1999).
86. S. M. Rezende *et al.*, *Phys. Rev. Lett.* **84**, 4212 (2000).
87. J. A. Katine *et al.*, *Phys. Rev. Lett.* **84**, 3149 (2000).
88. W. Weber, S. Riesen, H. C. Siegmann, *Science* **291**, 1015 (2001).
89. D. D. Awschalom, J. M. Kikkawa, *Phys. Today* **52**, 33 (1999).
90. J. M. Kikkawa, D. D. Awschalom, I. P. Smorchkova, N. Samarth, *Science* **277**, 1284 (1997).
91. J. M. Kikkawa, D. D. Awschalom, *Phys. Rev. Lett.* **80**, 4313 (1998).
92. ———, *Nature* **397**, 139 (1999).
93. J. A. Gupta, X. Peng, A. P. Alivisatos, D. D. Awschalom, *Phys. Rev. B* **59**, R10421 (1999).
94. M. Flatté, J. Byers, *Phys. Rev. Lett.* **84**, 4220 (2000).
95. Y. Ohno *et al.*, *Phys. Rev. Lett.* **83**, 4196 (1999).
96. I. Malajovich *et al.*, *Phys. Rev. Lett.* **84**, 1015 (2000).
97. I. Malajovich *et al.*, *Nature* **411**, 770 (2001).
98. B. Beschoten *et al.*, *Phys. Rev. B* **63**, R121202 (2001).
99. S. A. Crooker *et al.*, *Phys. Rev. Lett.* **75**, 505 (1995).
100. R. Fiederling *et al.*, *Nature* **402**, 787, (1999).
101. B. T. Jonker *et al.*, *Phys. Rev. B* **62**, 8180 (2000).
102. Y. Ohno *et al.*, *Nature* **402**, 790 (1999).
103. S. Koshihara *et al.*, *Phys. Rev. Lett.* **78**, 4617 (1997).
104. D. P. DiVincenzo *et al.*, *Nature* **408**, 339 (2000).
105. J. M. Kikkawa, D. D. Awschalom, *Science* **287**, 473 (2000).
106. G. Salis *et al.*, *Phys. Rev. Lett.* **86**, 2677 (2001).
107. R. K. Kawakami *et al.*, *Science* **294**, 131 (2001).
108. D. Loss, D. P. DiVincenzo, *Phys. Rev. A* **57**, 120 (1998).
109. G. Burkard, H. Engel, D. Loss, *Fortschr. Phys.* **48**, 965 (2000).
110. H.-A. Engel, D. Loss, *Phys. Rev. Lett.* **86**, 4648 (2001).
111. A. Imamoglu *et al.*, *Phys. Rev. Lett.* **83**, 4204, (1999).
112. N. H. Bonadeo *et al.*, *Science* **282**, 1473 (1998).
113. N. Paillard *et al.*, *Phys. Rev. Lett.* **86**, 1634 (2001).
114. J. A. Gupta *et al.*, *Science* **292**, 2458 (2001).
115. B. Kane, *Nature* **393**, 133 (1998).
116. R. Vrijen *et al.*, *Phys. Rev. A* **62**, 012306, (2000).
117. J. P. Gordon, *Phys. Rev. Lett.* **1**, 368 (1958).
118. M. A. Korotini *et al.*, *Phys. Rev. Lett.* **80**, 4305 (1998).
119. S. Watts, private communication.
120. J. M. Kikkawa *et al.*, *Physica E* **9**, 194 (2001).

121. This article was motivated in part from a WTEC study on Spin Electronics sponsored by the Defense Advanced Research Projects Agency, the NSF, Office of the Secretary of Defense, and National Institute of Standards and Technology.

REVIEW

Spin Ice State in Frustrated Magnetic Pyrochlore Materials

Steven T. Bramwell[1] and Michel J. P. Gingras[2,3]*

A frustrated system is one whose symmetry precludes the possibility that every pairwise interaction ("bond") in the system can be satisfied at the same time. Such systems are common in all areas of physical and biological science. In the most extreme cases, they can have a disordered ground state with "macroscopic" degeneracy; that is, one that comprises a huge number of equivalent states of the same energy. Pauling's description of the low-temperature proton disorder in water ice was perhaps the first recognition of this phenomenon and remains the paradigm. In recent years, a new class of magnetic substance has been characterized, in which the disorder of the magnetic moments at low temperatures is precisely analogous to the proton disorder in water ice. These substances, known as spin ice materials, are perhaps the "cleanest" examples of such highly frustrated systems yet discovered. They offer an unparalleled opportunity for the study of frustration in magnetic systems at both an experimental and a theoretical level. This article describes the essential physics of spin ice, as it is currently understood, and identifies new avenues for future research on related materials and models.

Competing or frustrated interactions are a common feature of condensed matter systems. Broadly speaking, frustration arises when a system cannot, because of local geometric constraints, minimize all the pairwise interactions simultaneously (*1*). In some cases, the frustration can be so intense that it induces novel and complex phenomena. Frustration is at the origin of the intricate structure of molecular crystals, various phase transitions in liquid crystals, and the magnetic domain structures in ferromagnetic films. It has also been argued to be involved in the formation of the stripelike structures observed in cuprate high-temperature superconductors. The concept of frustration is a broad one that extends beyond the field of condensed matter physics. For example, the ability of naturally occurring systems to "resolve" frustrated interactions has been argued to have bearings on life itself, exemplified by the folding of a protein to form a single and well-prescribed structure with biological functionality.

[1]Department of Chemistry, University College London, 20 Gordon Street, London WC1H 0AJ, UK. [2]Department of Physics, University of Waterloo, Waterloo, Ontario, N2L-3G1, Canada. [3]Canadian Institute for Advanced Research, 180 Dundas Street, Toronto, Ontario M5G 1Z8, Canada.

*To whom correspondence should be addressed. E-mail: gingras@gandalf.uwaterloo.ca.

Historically, the first frustrated system identified was crystalline ice, which has frozen-in disorder remaining down to extremely low temperature, a property known as residual, or zero-point entropy. In 1933, Giauque and co-workers accurately measured this entropy (*2*, *3*), enabling Pauling to offer his now famous explanation in terms of the mismatch between the crystal symmetry and the local bonding requirements of the water molecule (*4*). He predicted a special type of proton disorder that obeys the so-called "ice rules." These rules, previously proposed by Bernal and Fowler (*5*), require that two protons are near to and two are further away from each oxide ion, such that the crystal structure consists of hydrogen-bonded water molecules, H_2O (see Fig. 1). Pauling showed that the ice rules do not lead to order in the proton arrangement but rather, the ice ground state is "macroscopically degenerate." That is to say, the number of degenerate, or energetically equivalent proton arrangements diverges exponentially with the size of the sample. Pauling estimated the degeneracy to be $\sim(3/2)^{N/2}$, where N is the number of water molecules, typically $\sim 10^{24}$ in a macroscopic sample. This leads to a disordered ground state with a measurable zero-point entropy S_0 related to the degeneracy: $S_0 \approx (R/2)\ln(3/2)$, where R is the molar gas constant. Pauling's estimate of S_0 is very close to the most accurate modern estimate (*6*) and consistent with experiment (*2*). The disordered ice-rules proton arrangement in water ice was eventually